Catalysis Today 138 (2008) 183–186

Contents lists available at ScienceDirect

Catalysis Today

journal homepage: www.elsevier.com/locate/cattod

Steam reforming of ethanol over Pt–Ni Catalysts

Fatma Soyal-Baltacıoğlu, A. Erhan Aksoylu, Z. Ilsen Önsan [*]

Department of Chemical Engineering, Boğaziçi University, Bebek 34342, Istanbul, Turkey

ARTICLE INFO

Article history:
Available online 21 July 2008

Keywords:
Ethanol steam reforming
Hydrogen production
Pt–Ni catalysts
Kinetics

ABSTRACT

A parametric study was conducted over Pt–Ni/δ-Al_2O_3 to explore the effect of Pt and Ni contents on the ethanol steam reforming characteristics of the bimetallic catalyst. Experiments with catalysts having 0.2–0.3 wt%Pt and 10–15 wt%Ni contents indicated that the best ethanol steam reforming performance is achieved over 0.3 wt%Pt–15 wt%Ni/δ-Al_2O_3. Kinetics of ethanol steam reforming was studied over this catalyst in the 673–823 K interval using differential and integral methods of data analysis. A power-function rate expression was obtained with reaction orders of 1.01 and −0.09 in ethanol and steam, respectively, and the apparent activation energy of ethanol steam reforming over 0.3 wt%Pt–15 wt%Ni/δ-Al_2O_3 was calculated as 59.3 ± 2.3 kJ mol^{-1}.

1. Introduction

Environmental problems arising from the extensive use of fossil fuels and dwindling petroleum reserves have increased the search for diverse energy sources. Among the alternatives at hand, the use of hydrogen as a fuel is projected to reduce air pollution and greenhouse gas emissions significantly, and the proton-exchange membrane (PEM) fuel cell fuelled by pure hydrogen is currently the leading candidate for various stationary and mobile applications. Although natural gas, LPG, gasoline and methanol are generally regarded as the sources for hydrogen, ethanol has also attracted some attention in recent years [1–3]. Ethanol is a renewable resource that is easier to store, safer to handle and transport owing to its lower toxicity and volatility compared to methanol. Chemical storage of hydrogen in liquid fuels is considered to be an advantageous option for delivering hydrogen. Steam reforming (SR) has the highest efficiency for hydrogen production among other alternatives such as partial oxidation or auto-thermal reforming; the only inconvenience is its highly endothermic nature [4]. The reforming of oxygenated hydrocarbons (methanol and ethanol) requires considerably less energy per mole of H_2 formed than the reforming of saturated hydrocarbons and produces mostly CO_2 [5].

$$C_2H_5OH + 3H_2O \Rightarrow 2CO_2 + 6H_2, \quad \Delta H^{\circ}_{298} = 173\,\mathrm{kJ\,mol^{-1}} \qquad (1)$$

Investigation of hydrogen production from ethanol is fairly new. Ethanol SR proceeds at higher temperatures (350–900 °C) compared to methanol SR (200–400 °C) on account of its C–C bond, and at relatively high water-to-ethanol ratios. Recent reviews of ethanol SR emphasize the significant effects of the type of catalyst, method of catalyst preparation and reaction conditions on ethanol conversion, hydrogen production and product distribution [1,2]. Base metals such as Ni, Co, Ni–Cu and noble metals such as Pt, Pd and Rh over appropriate supports show potential for ethanol SR, and the main problems to be tackled are byproduct formation and coke deposition. Side products observed on Ni-based catalysts are mainly CH_4 and CO_x formed by ethanol SR with methane production, ethanol decomposition, methane SR or methanation depending on the reaction temperature [6]. Al_2O_3 and CeO_2-supported noble metal catalysts were studied by FTIR, TPD and TPR methods to clarify possible reaction mechanisms, and it was reported that ethylene, resulting from ethanol dehydration, is typically formed over Al_2O_3-supported noble metals, while considerable acetaldehyde, resulting from ethanol dehydrogenation, is also formed on CeO_2-supported catalysts [7]. Deactivation by carbon formation was observed on Rh/CeO_2–ZrO_2, but total regeneration was possible at low temperatures [8]. Reports on intrinsic kinetics of ethanol SR over Ni and Ru catalysts include power-law rate expressions where ethanol consumption rate is first order with respect to ethanol and independent of steam [1,9,10].

Pt–Ni catalysts are efficient for the auto-thermal reforming (ATR) of hydrocarbon feeds and are potential candidates for energy efficient commercial processes [11]. ATR is a combination of total oxidation and SR along with high-temperature water-gas shift, and eliminates the need for an external source of heat. Kinetics of ATR is described by the simultaneous use of separate rate expressions for total oxidation and SR of the hydrocarbon fuel as well as a third rate equation for the concurrent water-gas shift. Computer simulations based on the thermodynamic analysis of a fuel processor utilizing

---

[*] Corresponding author. Tel.: +90 212 359 6412; fax: +90 212 287 2460.
E-mail address: onsan@boun.edu.tr (Z.I. Önsan).

0920-5861/$ – see front matter © 2008 Elsevier B.V. All rights reserved.
doi:10.1016/j.cattod.2008.05.035

ethanol and comprising ATR, low-temperature water-gas shift and selective CO oxidation reactors showed that the H_2 yields obtained match up to about 65% of the theoretical [12]. Ethanol SR experiments over 0.2 wt%Pt–15 wt%Ni/δ-Al_2O_3 at 673–823 K demonstrated that the bimetallic catalyst was resistant to carbon formation even at water-to-ethanol ratios as low as 3.0, side products detected were CH_4 and CO_x, and ethanol conversion rates were directly proportional to ethanol partial pressure and slightly inhibited by steam partial pressure [13].

The present work contains a series of experiments conducted over Pt–Ni/δ-Al_2O_3 catalysts with different Pt and Ni contents in order to select the most suitable Pt–Ni catalyst on which ethanol SR proceeds well and is coupled with a kinetic study to extract the rate expression for describing ethanol SR kinetics in the simulation of ATR units of fuel processors.

2. Experimental work

2.1. Catalyst preparation

Pt–Ni/δ-Al_2O_3 catalysts having different Pt (0.2–0.3 wt%) and Ni (10–15 wt%) loadings were prepared by drying γ-Al_2O_3 at 423 K and calcination at 1173 K to obtain thermally stable δ-Al_2O_3, followed by sequential incipient-to-wetness impregnation using aqueous $Ni(NO_3)_2{\cdot}6H_2O$ (Merck) and $Pt(NH_3)_4(NO_3)_2$ (Aldrich) solutions, respectively, with an intermediate calcination at 873 K and a final calcination at 773 K [14]. The BET surface area of the δ-Al_2O_3 support was determined as 82 $m^2\,g^{-1}$ using a Micromeritics Flowsorb II apparatus. The catalysts tested were 0.2 wt%Pt–10 wt%Ni, 0.3 wt%Pt–10 wt%Ni, 0.2 wt%Pt–15 wt%Ni and 0.3 wt%Pt–15 wt%Ni.

2.2. Reaction experiments

Experiments were conducted at atmospheric pressure and 673–823 K in 4-mm i.d. stainless steel fixed-bed down-flow microreactors located in the center of a well-insulated 2.5-cm i.d. furnace tube with 50 cm length and having a constant temperature zone of about 30 cm and controlled to ±0.1 K by a Shimaden FP-21 programmable controller. Reaction temperatures were measured just outside the 4-mm i.d. reactor tube with a thermocouple adjacent to the catalyst bed. Before the steam reforming reaction was started, fresh catalyst samples were reduced under 20 $cm^3\,min^{-1}$ pure hydrogen flow at 773 K for 4 h and then the reaction temperature was adjusted under inert N_2 flow. Flow rates of H_2 and N_2 gases were monitored by calibrated Omega Model 5878 and Aalborg GFC171S mass flow controllers. Liquid water–ethanol feed mixtures were evaporated into a preheated diluent N_2 stream using a Jasco PU-1580 intelligent HPLC pump and mixed to ensure homogeneity prior to microreactor inlet. Liquid flow rates metered on the pump were converted into gas flow rates by using ideal gas law (normalized to 298 K and 1 atm), molecular weights, liquid densities and water-to-ethanol ratios [14]. All connecting lines were kept at 423 K to prevent condensation. Two gas chromatographs, Shimadzu GC-14A and Shimadzu GC-8A, with Porapak Q and Molecular Sieve 5A columns and TCDs, respectively, were used for the analyses.

In parametric experiments, 20 mg of 250–422 μm fresh catalyst particles were diluted with inert δ-Al_2O_3 to a total bed weight of 250 mg. Preliminary experiments showed that δ-Al_2O_3 and the stainless steel reactor were inert, and external–internal mass transfer resistances were negligible [13]. The microreactor was operated with an initial ethanol concentration of 6.25 vol.%, a water-to-ethanol ratio of 6.0 and a space time (W_{cat}/F_{EtOH}) of 80 mg s mL^{-1}, for comparing catalyst performances at 673–823 K. All samples were tested up to 375 min time-on-stream (TOS); stable ethanol conversion levels were attained after 200 min TOS and data obtained at 300 min TOS were used in catalyst comparisons. Before starting kinetic experiments, the 0.3 wt%Pt–15 wt%Ni sample was tested up to 420 min TOS at 723 K with a stable ethanol conversion level. Kinetic experiments were conducted at 1 atm and 723 K, over 10–40 mg of fresh catalyst samples diluted with inert δ-Al_2O_3 to 250 mg, using inlet ethanol concentrations of 5.0–7.0–9.0 vol.%, water-to-ethanol molar ratio of 6.0 and space times (W_{cat}/F_{EtOH}) of 50–200 mg s mL^{-1} (0.33–1.32 g h mol^{-1}). The temperature dependence of the rate constant was determined at five temperatures in the 673–823 K range, using initial ethanol and water concentrations of 7.0 vol.% and 42.0 vol.%, respectively, and space times of 0.33–1.0 g h mol^{-1}. Ethanol conversion data obtained at 375 min TOS were used in the evaluation of kinetic parameters. Deactivation or coke formation was not observed within the range of conditions used in this study.

Ethanol conversion and hydrogen yield were defined as mole of ethanol consumed per mole of ethanol in feed and mole of H_2 formed per mole of ethanol in feed, respectively. In kinetic measurements, ethanol SR rates were calculated as follows:

$$(-r_{EtOH}) = \frac{dx_{EtOH}}{d(W_{cat}/F_{EtOH_{in}})} \tag{2}$$

where x_{EtOH} is fractional ethanol conversion, $F_{EtOH_{in}}$ is ethanol flow rate in the feed in mol h^{-1}, W_{cat} is catalyst weight in g and $(-r_{EtOH})$ is the reaction rate in mol $g^{-1}\,h^{-1}$. Ethanol SR rates were obtained from the slopes of the tangents to the x_{EtOH} versus $W/F_{EtOH_{in}}$ curves at various points, using curves constructed from the data of at least six separate experiments for each feed composition.

3. Results and discussion

3.1. Effect of catalyst composition

The effect of catalyst composition was initially tested at 723 K with a constant space time of 80 mg s mL^{-1} (or 0.53 g h mol^{-1}) over catalyst samples with 0.2–0.3 wt%Pt and 10–15 wt%Ni loading. Initial ethanol and water concentrations were kept constant at 6.25 vol.% and 37.5 vol.%, respectively. Figs. 1 and 2 indicate that catalysts with 15 wt% Ni loading are better in terms of both ethanol conversion and H_2 production at 723 K, probably due to better dispersion and abundance of Ni sites promoting the reforming reaction. Previous work conducted by our group on SEM-BCI and EDX analyses of δ-Al_2O_3 supported 0.2 wt%Pt, 15 wt%Ni and 0.2 wt%Pt–15 wt%Ni catalysts indicated that a 15 wt%Ni content uniformly covers the support surface [15].

The same SEM-BCI and EDX study also showed that while Pt is well dispersed on the δ-Al_2O_3 support of the 0.2 wt%Pt catalyst with Pt particle sizes in the 10–60 nm range, Pt clusters 70–330 nm in size are nestled over the 15 wt%Ni environment covering the

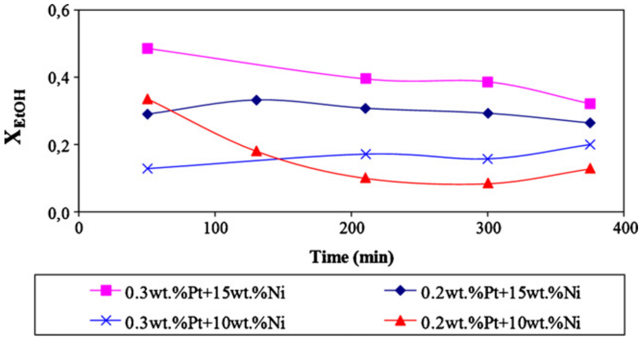

Fig. 1. Effect of metal loading on ethanol conversion at 723 K.

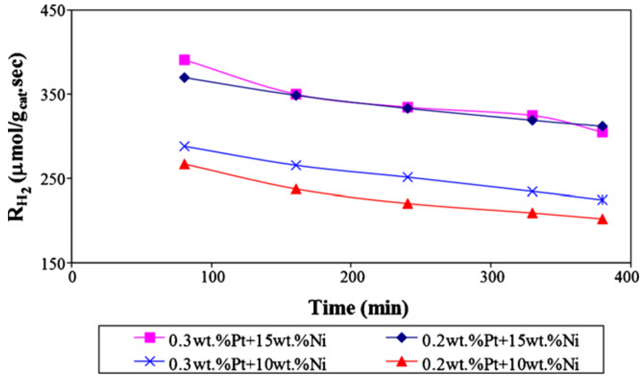

Fig. 2. Effect of metal loading on hydrogen production at 723 K.

support surface of 0.2 wt%Pt–15 wt%Ni [15]. In the present study, higher Pt content improves ethanol conversion capabilities of catalysts with 15 wt% and 10 wt% Ni, the improvement in H_2 production rates of 10 wt% Ni-containing catalysts being more noticeable at 723 K. It may be speculated that this enhancement in catalytic activity is attributable to an improvement in Ni dispersion caused by the presence of Pt especially on catalysts with lower Ni content.

The effect of temperature was studied at 673–823 K on catalysts with 15 wt% Ni. The difference in the ethanol conversions of samples with 0.2 wt% and 0.3 wt% Pt was found to increase with temperature in favor of 0.3 wt% Pt and reach its maximum at 773 K (Fig. 3). The corresponding H_2 production rates (data not shown) measured on 0.2 wt%Pt–15 wt%Ni were much lower (ca. 50 μmol g s^{-1}) at 673 K but increased quickly until 723 K to match the H_2 production rate of 0.3 wt%Pt–15 wt%Ni and then stayed constant up to 823 K. On the other hand, H_2 production over 0.3 wt%Pt–15 wt%Ni increased drastically with temperature from about 175 μmol g s^{-1} at 673 K to 485 μmol g s^{-1} at 773 K and stayed constant until 823 K.

The CH_4 production rate increased only slightly from 8.1 μmol g s^{-1} to 8.6 μmol g s^{-1} in the entire 673–823 K range. The highest CH_4 production rate of 9.2 μmol g s^{-1} was obtained over 0.2 wt%Pt–15 wt%Ni at 732 K. The H_2/CH_4 production ratios (point selectivity values) presented in Fig. 4 indicate that the performance of 0.3 wt%Pt–15 wt%Ni is better at all temperatures with a maximum point selectivity of almost 60 at 773 K. The highest H_2/CO point selectivity is also observed for 0.3 wt%Pt–15 wt%Ni at 773 K; however, both H_2/CO and CO_2/CO production ratios decline as the temperature rises from 773 K to 823 K (Fig. 5). Decreases in the H_2/CO and CO_2/CO point selectivities may be explained by the information that the steam reforming of oxygenated hydrocarbons produces mostly CO_2 some of which is later converted to CO by the rapid reverse-water-gas shift reaction that occurs at high H_2 concentrations [3,5]. Taking all observations into account, it may be said that ethanol SR with CO_2 and CH_4 formation is important at 723 K over both catalysts; at higher temperatures, the distinctive properties of Ni are modified by the increasing Pt content to accommodate methane SR and water-gas shift reactions.

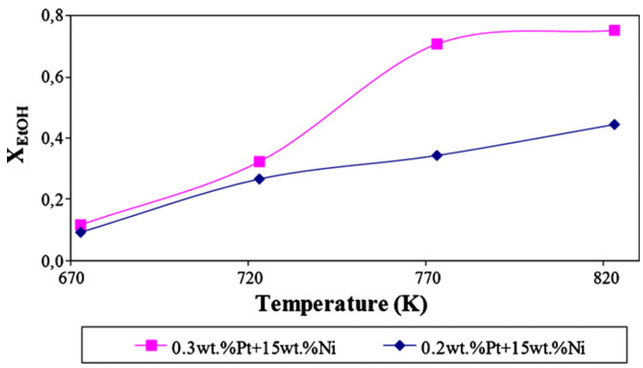

Fig. 3. Effect of temperature on ethanol conversion (300 min time-on-stream).

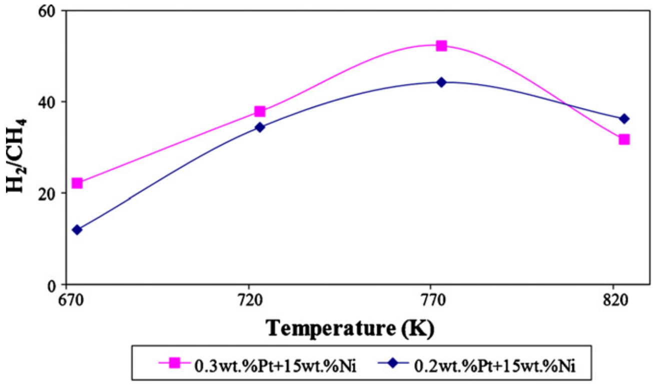

Fig. 4. Effect of temperature on H_2/CH_4 point selectivities (300 min time-on-stream).

3.2. *Kinetics of ethanol SR over 0.3 wt%Pt–15 wt%Ni/δ-Al_2O_3*

Kinetic data were obtained at 723 K using three different ethanol (5–7–9 vol.%) and steam (30–42–54 vol.%) compositions at six different space times each (Fig. 6). Ethanol SR rates were evaluated from integral reactor data obtained under isothermal conditions by numerical differentiation of the x_{EtOH} versus $W/F_{EtOH_{in}}$ curves to calculate individual reaction rates at all space times and also by extrapolation back to zero space time to calculate initial rates. Ethanol conversion data obtained at 375 min TOS were used in the evaluation of kinetic parameters. Data were processed by nonlinear regression in the MATLAB environment using the Levenberg–Marquardt algorithm and the power-function rate expression of the following equation:

$$-r_{C_2H_5OH} = \left[k_0 \exp\left(-\frac{E_A}{RT}\right)\right](P_{C_2H_5OH})^{\alpha}(P_{H_2O})^{\beta} \qquad (3)$$

The rate parameters estimated are given in Table 1. Fig. 7 demonstrates the agreement between model-predicted and experimentally measured ethanol SR rates within the range of

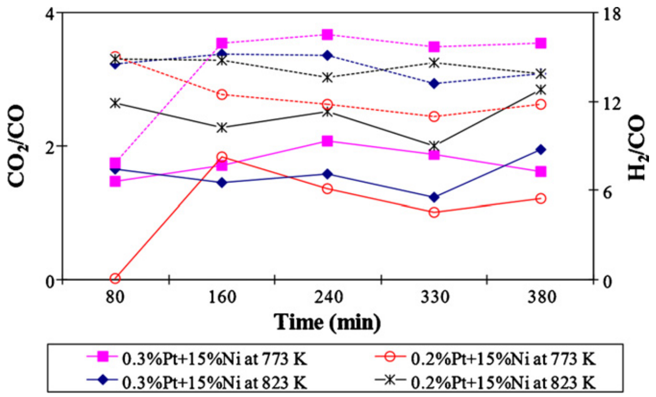

Fig. 5. Effect of temperature and time-on-stream on CO_2/CO and H_2/CO point selectivities (solid lines and left *y*-axis indicate CO_2/CO selectivity, dotted lines and right *y*-axis indicate H_2/CO selectivity).

Table 1
Kinetic parameters of ethanol SR over 0.3 wt%Pt–15 wt%Ni/δ-Al_2O_3 (673–823 K)

Parameter	Units	Estimates
α		1.01 ± 0.03
β		−0.09 ± 0.02
k	mol g cat^{-1} h^{-1} atm$^{-0.92}$	9.23 ± 0.3
E_A	kJ mol^{-1}	59.3 ± 2.3

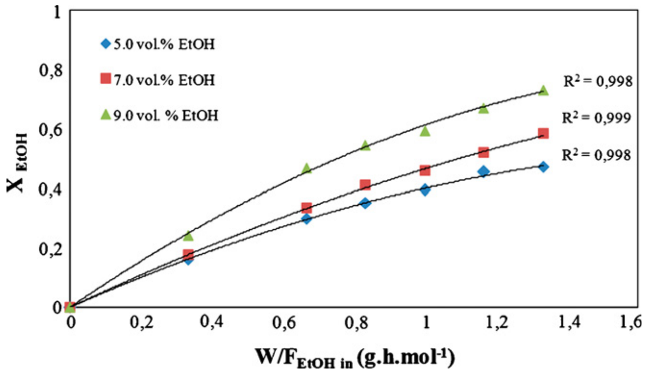

Fig. 6. Effects of feed composition and space time on ethanol conversion at 723 K and 375 min time-on-stream.

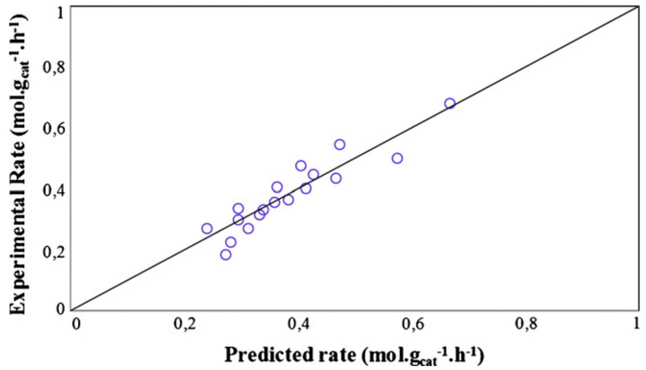

Fig. 7. Comparison of model-predicted and experimentally measured ethanol SR rates at 723 K.

conditions tested (Fig. 7). The positive first-order dependence on ethanol was also confirmed by neglecting the mild inhibition of −0.09 by steam partial pressure and using the integral method with a reasonably good fit of $R^2 = 0.97$ to a plot of $\ln(1 - x_{EtOH})$ versus (W/F_{total}).

Ethanol SR rates obtained in the same manner as described above at five different temperatures between 673 K and 823 K and fixed feed composition (7.0 vol.% and 42.0 vol.% ethanol and water, respectively) and Eq. (3) were used to calculate the five rate constants (k values) required for estimating the activation energy (E_A) of the Arrhenius functionality. The apparent E_A of ethanol steam reforming over 0.3 wt%Pt–15 wt%Ni/δ-Al_2O_3 was calculated as 59.3 ± 2.3 kJ mol^{-1} (Fig. 8).

The reaction orders of 1.01 ± 0.03 for ethanol and −0.09 ± 0.02 for steam are in agreement with those obtained previously [13] on 0.2 wt%Pt–15 wt%Ni/δ-Al_2O_3 at 673 K (1.25 ± 0.05 and −0.215 ± 0.05, respectively) to the extent that a positive order close to unity and a mildly negative order are obtained for ethanol and steam partial pressures. These reaction orders would indicate the presence of adsorbed water on the catalyst surface and a surface reaction involving relatively weakly adsorbed ethanol. An increase in the Pt content from 0.2 wt% to 0.3 wt% seems to strengthen ethanol adsorption to some extent, thus diminishing the surface coverage of water. The increase observed in the apparent E_A values (59.3 kJ mol^{-1} as compared to 39.3 kJ mol^{-1} for 0.3 wt% and 0.2 wt% Pt-containing catalysts, respectively) would also support this explanation.

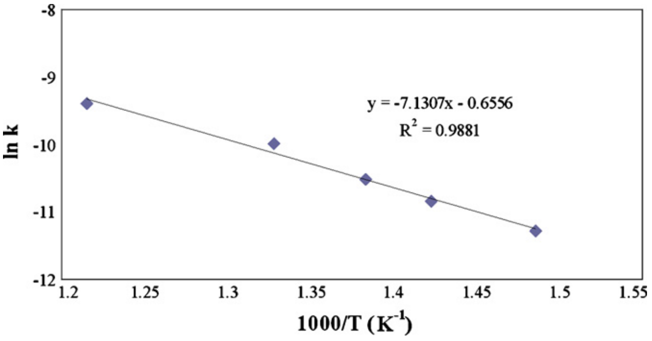

Fig. 8. Arrhenius plot of ethanol SR over 0.3 wt%Pt–15 wt%Ni/δ-Al_2O_3.

4. Conclusions

Studies conducted on bimetallic Pt–Ni/δ-Al_2O_3 with different compositions indicate that catalysts with Ni loading of 15 wt% are more efficient in ethanol SR and that a higher Pt content of 0.3 wt% is successful in promoting H_2 production as well as H_2/CH_4 and H_2/CO point selectivity. Ethanol SR performance of 0.3 wt%Pt–15 wt%Ni/δ-Al_2O_3 is better in terms of both ethanol conversion and selectivity towards hydrogen production up to 773 K. The power-function rate expression proposed on the basis of an extensive kinetic study for determining intrinsic reaction rates at 723 K from integral reactor data under conditions extending up to about 70% ethanol conversion has reaction orders of 1.01 and −0.09 in ethanol and steam partial pressures, respectively, and can reliably be used for simulating ethanol SR or the SR component of ethanol ATR. The apparent activation energy of ethanol steam reforming over 0.3 wt%Pt–15 wt%Ni/δ-Al_2O_3 in the 673–823 K interval is calculated as 59.3 ± 2.3 kJ mol^{-1}.

Acknowledgements

This research was supported by the TUBITAK project 104M163 and by the Boğaziçi University Research Fund projects BAP-06HA501 and DPt-07K120630. TUBA-GEBIP grant to A.E. Aksoylu is also acknowledged.

References

[1] P.D. Vaidya, A.E. Rodrigues, Chem. Eng. J. 117 (2006) 39.
[2] A. Haryanto, S. Fernando, N. Murali, S. Adhikari, Energy Fuels 19 (2005) 2098.
[3] Z.I. Önsan, Turk. J. Chem. 31 (2007) 531.
[4] D.L. Trimm, Z.I. Önsan, Catal. Rev. Sci. Eng. 43 (2001) 31.
[5] T.A. Semelsberger, L.F. Brown, R.L. Borup, M.A. Inbody, Int. J. Hydrogen Energy 29 (2004) 1047.
[6] J. Comas, F. Marino, M. Laborde, N. Amadeo, Chem. Eng. J. 98 (2004) 61.
[7] A. Erdohelyi, J. Rasko, T. Kecskes, M. Toth, M. Dömök, K. Baan, Catal. Today 116 (2006) 367.
[8] H.-S. Roh, A. Platon, Y. Wang, D.L. King, Catal. Lett. 110 (2006) 1.
[9] J. Sun, X.-P. Qiu, F. Wu, W.-T. Zhu, Int. J. Hydrogen Energy 30 (2005) 437.
[10] P.D. Vaidya, A.E. Rodrigues, Ind. Eng. Chem. Res. 45 (2006) 6618.
[11] B.S. Caglayan, A.K. Avci, Z.I. Önsan, A.E. Aksoylu, Appl. Catal. A Gen. 280 (2005) 181.
[12] E. Örücü, M. Karakaya, A.K. Avci, Z.I. Önsan, J. Chem. Technol. Biotechnol. 80 (2005) 1103.
[13] E. Örücü, F. Gökaliler, A.E. Aksoylu, Z.I. Önsan, Catal. Lett. 120 (2008) 198.
[14] A.K. Avci, D.L. Trimm, A.E. Aksoylu, Z.I. Önsan, Appl. Catal. A. Gen. 258 (2004) 235.
[15] A.K. Avci, D.L. Trimm, A.E. Aksoylu, Z.I. Önsan, Catal. Lett. 88 (2003) 17.